INITIAL RESULTS FROM FERMILAB'S VERTICAL TEST STAND FOR SRF CAVITIES*

J. P. Ozelis#, R. Carcagno, C. M. Ginsburg, Y. Huang, R. Nehring, B. Norris, V. Poloubotko, R. Rabehl, I. Rakhno, C. Reid, T. Peterson, D. A. Sergatskov, C. Sylvester, M. Wong, C. Worel, A. Yuan, Fermilab, Batavia, IL. 60510, U.S.A.
C. Grenoble, T. J. Powers, TJNAF, Newport News, VA. 23606, U.S.A.

Abstract

Fermilab has constructed a facility for vertical testing of SRF cavities, operating at a nominal temperature of 2K, to be used as part of the global International Linear Collider (ILC) effort to improve cavity processing and performance reproducibility. Following successful cryogenic commissioning, the first tests of single cell and 9-cell ILC-style cavities were performed. These first test results are presented in detail, along with a brief discussion of present measurement accuracy.

INTRODUCTION

The Vertical Cavity Test Facility (VCTF) at Fermilab is designed to test SRF cavities at a nominal frequency of 1.3GHz in a 2K LHe bath, and will support up to 48 cavity tests per year in single-cavity test mode. The VCTF has been designed to accommodate two 9-cell cavities as a means of increasing throughput to 80 cavity tests/year. The VCTF facility includes RF and DAQ systems, radiation shielding, a system of interlocks for personnel protection, and is connected to an existing cryoplant and vacuum system allowing VCTF operations down to 1.5K. Complete design details have been presented elsewhere [1][2], along with cryo commissioning experience [3] and upgrade plans to incorporate diagnostics and increase cavity test throughput to 200 test cycles/year [1][4] .

INITIAL CAVITY TEST RESULTS

Singe Cell Cavity Tests

The first opportunity to perform a test of a superconducting cavity at 2K in the VCTF was with a single-cell cavity fabricated at Jefferson Lab (JLab). The cavity was made of half-cells deep drawn from large grain niobium sheets obtained from Ningxia OTIC, then electron-beam welded in the customary manner. The cavity was fitted with plain beam tubes. The cavity was processed (BCP), high pressure rinsed, assembled, and initially tested at JLab [6]. Before shipment to Fermilab, the cavity was given a light BCP treatment, high pressure rinsed, assembled, evacuated, and then hermetically sealed at JLab. Upon arrival at Fermilab the cavity was mounted onto the test stand using a temporary support structure consisting of 2 G-10 discs that support the cavity below the cell and upper beamline flange. The cavity was then inserted into the VCTF Dewar and cooled down to 2K. No active pumping was performed on this cavity during cryogenic RF testing. The cavity was equipped with a fixed input coupler with a measured Q_{ext} of 1.5 x 10^{10}.

After the RF signal distribution network was calibrated and cable attenuations measured per standard procedures (see, e.g., the comprehensive process described in [5]), RF power was slowly increased and measurements of gradient and Q_0 were performed until a multipacting barrier appeared at a gradient of about 6-7 MV/m, which was accompanied by radiation. After a short while this barrier was breached through CW processing (holding the incident RF power slightly above the MP threshold), and re-appeared at about 10-11 MV/m, again accompanied by radiation. This barrier was almost immediately breached, but FE remained at gradients above 12 MV/m. This field emission processed away, re-appearing at higher gradients (>17MV/m), and leading to a field emission (FE) induced thermal breakdown at 26 MV/m. After subsequent CW and pulse processing the cavity reached a gradient of 27.4MV/m, still accompanied by some FE (~30-35 mR/hr). The cavity's Q_0 vs E behavior and radiation observations are shown in Figs. 1 and 2.

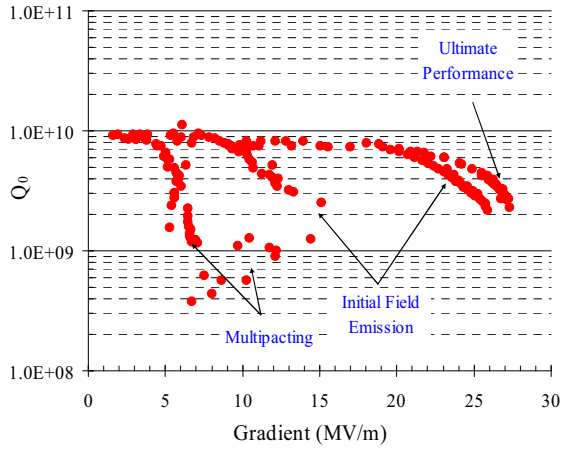

Figure 1: Q_0 vs E curve of the large-grain single cell cavity. The effect of the multipacting barriers on the cavity Q_0 can be easily seen, along with the Q-drop from field emission at high gradients.

Of note is the low value of this cavity's low-field Q_0 (about 9 x 10^9). This is presumed to be a result of the higher background magnetic field in the test Dewar, due to the absence of the inner magnetic shielding, which was not yet available at the time of testing. This leads to a

*Operated by Fermi Research Alliance, LLC under Contract No. DE-AC02-07CH11359 with the United States Department of Energy.
#ozelis@fnal.gov

background field of about 50mG, significantly higher than both the design goal with the inner magnetic shield in place (<10mG), and the background field in the JLab Dewar where this cavity was previously tested. The additional surface resistance (~10nΩ) from this additional background field is sufficient to account for the change in observed low-field Q_0.

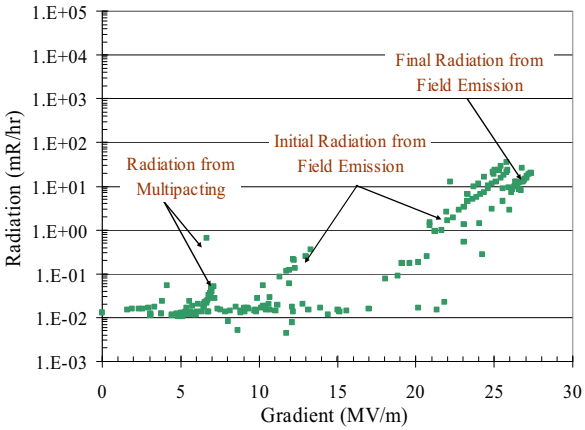

Figure 2: Observed radiation during test of large-grain single cell ILC cavity. The radiation corresponding to mulipacting can be seen at gradients of about 6-7 MV/m, with field emission initially beginning at 12MV/m and, after processing, re-appearing at ~17-18 MV/m.

During a series of tests at JLab, this cavity reached a maximum gradient of 33 MV/m with a Q_0 at that gradient of 1.14 x 10^{10}, a low-field Q_0 value of over 2 x 10^{10}, and was limited by quench [6]. Recall that before being sent to Fermilab, the cavity underwent a light BCP and an additional HPR cycle and was re-assembled. Upon arrival at Fermilab, it was found that the cavity vacuum had been degraded due to a leak, which was subsequently repaired and the cavity re-evacuated. As a result of these actions, and the higher background magnetic field in the Fermilab Dewar, the differences in performance observed at Fermilab and JLab are not unreasonable.

Initial Nine Cell Cavity Tests

The first nine-call cavity available for testing in the Fermilab VCTF was cavity AES01, a nine-cell ILC baseline design style cavity fabricated by Advanced Energy Systems (AES)[7] as part of the ILC-America's effort to develop domestic cavity vendors. This cavity was processed (EP) and tested numerous time at JLab, and consistently showed a quench limitation at gradients between 16-18MV/m, without field emission [8]. This performance was independent of number of EP processing cycles or total amount of Nb removal. Mode measurements made at JLab indicated that cells 3/7 were the likely candidates for the origin of this quench.

The primary goal for testing AES01 at Fermilab was to commission the VCTF RF and DAQ systems; however, the availability of the Fast Thermometry System (FTS) developed at Fermilab for previous SRF efforts [9] provided the opportunity to instrument the equators of cells 3 and 7 with 8 Cernox® Resistance Temperature Devices (RTD's) each, in an attempt to localize this quench origin. These RTD's were then read out using the FTS system during the initial tests of AES01.

The initial test plan was to simply measure the cavity's Q_0 vs E behavior at 2K. This was readily accomplished, and the results are shown in Fig. 3. The cavity was found to quench at a gradient of about 15.6MV/m, consistent with earlier results from JLab, and did not exhibit any field emission (see Fig. 4.). The Q-values as measured at Fermilab were significantly lower than those measured during similar tests at JLab. However, just as was the case for the single cell cavity test discussed earlier, the inner magnetic shielding of the Fermilab VCTF Dewar was not yet in place during these tests, resulting in a significantly higher background magnetic field (50mG) than that of the JLab Dewar (25-30mG). The difference in background field of 20-25mG translates to an increase in surface resistance of 5-7 nΩ, which can account for the degradation in Q_0 observed at Fermilab.

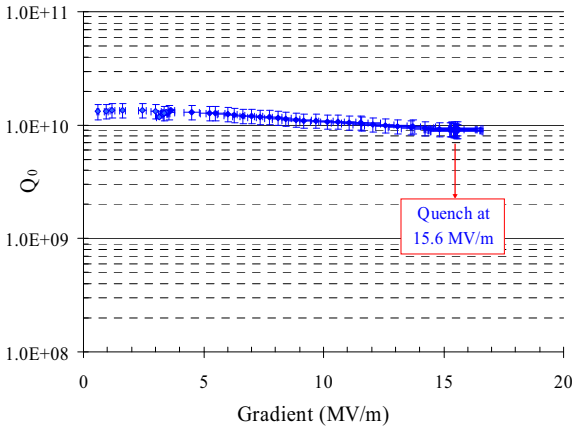

Figure 3: Q_0 vs E for cavity AES01. The cavity quenched reproducibly at 15.6MV/m.

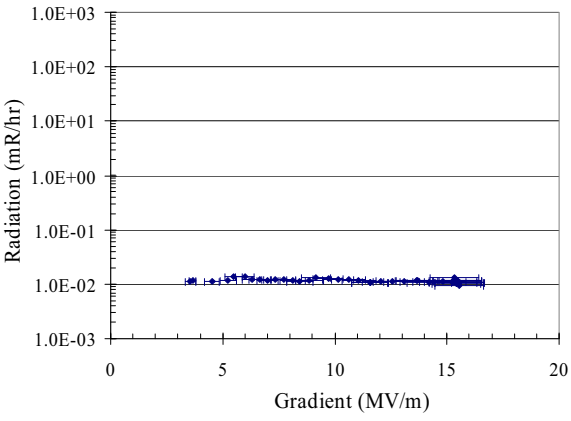

Figure 4: Radiation measured during the first test of cavity AES01 at the Fermilab VCTF. As can be seen from the data, the cavity did not exhibit any field emission.

A second measurement run was performed the day after this initial test, to assess reproducibility of the measurement system. No changes were made to the system configuration, the cavity was not thermally cycled, and cable calibrations were not performed. The results of this second run were virtually identical to the first, and well within the computed measurement errors. A third measurement run was performed several days after the second. This time, however, the cavity was partially thermally cycled and a full cable calibration was performed. Again the results were virtually identical and all three runs are shown together in Fig. 5. The agreement between these runs, and the previous test results from JLab, demonstrate the stability of the VCTF RF and DAQ system, and provide a reasonable level of confidence in the accuracy of the measurement system.

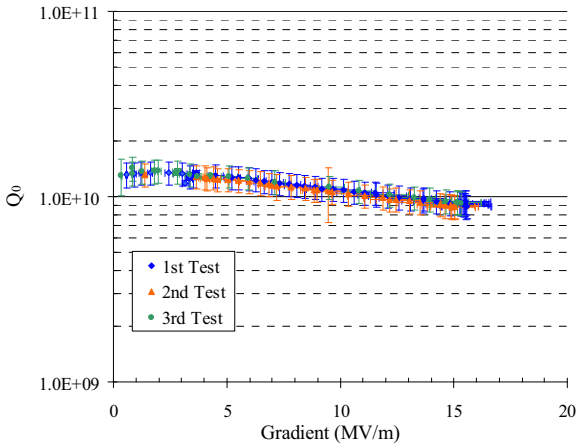

Figure 5: Q_0 vs E curves for the three initial test runs of cavity AES01 in the π-mode, showing excellent agreement between all three runs. These results also agree well with the latest test results from JLab.

Quench Localization in Cavity AES01

During the initial test runs discussed above, the Fast Thermometry System (FTS) was exercised. Readout of the RTD's during runs to quench conclusively determined that the origin of the quenches was confined to cell #7 (as numbered from the field-probe end of the cavity). Initial analysis of these data showed that RTD's # 5 and 6 on cell #7 exhibited strong thermal responses that were correlated to the cavity quench as indicated by the cavity transmitted power signal. No other sensors exhibited any response. The signals from sensors #5 & #6 were essentially uniform indicating that the quench origin was perhaps located equidistant between them.

After the first tests of AES01 with the FTS localized the quench origin to cell 7, the Dewar was then warmed up so that the cavity could be removed, and additional thermometry added to the region near the suspected quench origin in order to better localize it. A total of 8 single RTD's were mounted above and below the equator weld midline, in the area where RTD's #5 & #6 had been during the previous test run. These RTD's had an azimuthal spacing of a few mm, and were mounted in an interleaved fashion (alternating above/below the weld midplane, with the center of the sensor displaced about 5mm along the cavity axis from the weld midplane). An additional 8 RTD's were mounted as pairs on G-10 strips aligned with the beam axis (vertically) and placed outboard of the 8 single RTD's – 4 on each side. See Fig. 6 for details.

In subsequent test runs, scans of the RTD's were performed as the cavity was ramped to quench in the π-mode. During quenches a strong thermal response was observed on all of the equator weld sensors, as seen in Fig. 7. During these scans the strongest initial response was observed on sensors #3 & #4 (strongest on #3), which were placed above the equator weld, indicating the development and growth of a "hot-spot". Other nearby sensors only indicated moderate or minor temperature rises above background, until the quench (see Fig. 8). For example, the sensors immediately to the right (#1 & #2) and below (#5) sensors #3 & #4 show lower thermal response. This indicates that the quench origin is between sensors #3 and #4, (closer to #3) and possibly slightly above them – if it were below them, then the sensors directly beneath the gap between sensors #3 & #4 should also exhibit a strong response. This was not the case, and may be due to reduced thermal conductivity across the weld joint, or simply reflect the distance from the hot spot.

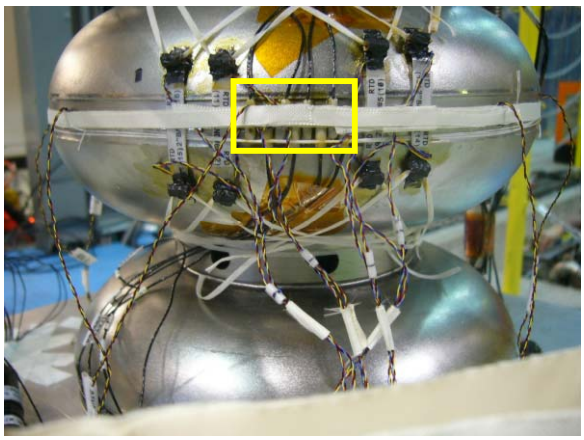

Figure 6: Layout of the additional RTD's used to localize the quench origin in cell #7. The RTD's outlined in the box are the 8 sensors located above and below the equator weld midplane. Outboard of them are the 4 G-10 strips with two sensors each, oriented vertically.

Additional runs to quench in other passband modes were performed, and only in those modes where there were high field levels in cells 3/7 were appreciable temperature rises observed, and once again primarily only in sensors #3 & #4. Smaller temperature rises were observed in many of the RTD's mounted on cell 7 when at high fields in the 7π/9 mode (which does not support high fields in cells 3/7); however, this mode exhibited significant FE which led to quench. Most likely the impact of the FE electrons on the cavity walls led to a

high local temperature rise (leading to the observed quench) and smaller associated global temperature rise (detected by the cell 7 RTD's).

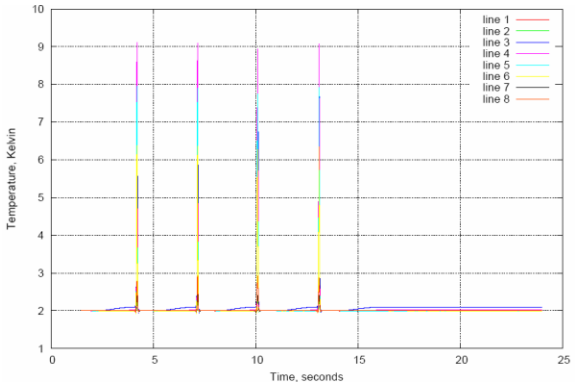

Figure 7: Response of the 8 midplane RTD's. The temperature "spikes" correlate with the quenching of the cavity. After the last quench, the hot-spot re-develops, but does not lead to a quench, probably as a result of a small drift in the RF phase of the incident power signal - which leads to a slightly lower cavity field (below the quench threshold), for the same level of incident power.

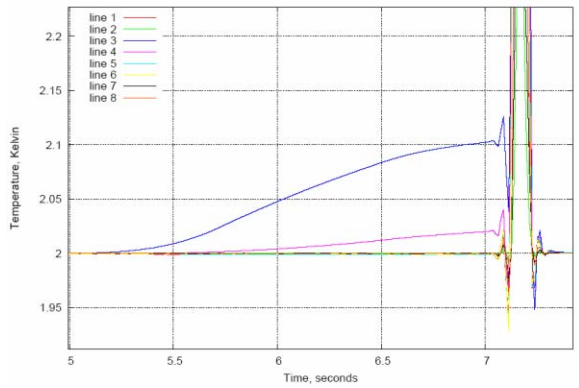

Figure 8: Response of the 8 RTD's placed above and below the equator weld midplane. Onset and development of the hot-spot can be observed in the response of sensors #3 and #4, with the strongest response for sensor #3. At the quench, all sensors showed a sharp increase.

Mode Measurements

As mentioned above, runs to quench were performed in all of the passband modes of the cavity (except for the π/9 mode). For each mode, the cavity input coupling was determined, along with calibration of the transmitted power (field) probe. Input power to the cavity was increased in each mode until a quench limit was observed. In the 7π/9 mode, the quench limit was determined to be due to FE. Pulse-processing was performed in this mode to reduce FE – after which the π-mode equivalent gradient improved from 14.6 MV/m to 19.4 MV/m. Measurements at the maximum limiting field for each mode are summarized in Table 1, and the relevant Q vs E curves are shown in Fig. 9. The FE data from operation in the 7π/9 mode is shown in Fig. 10.

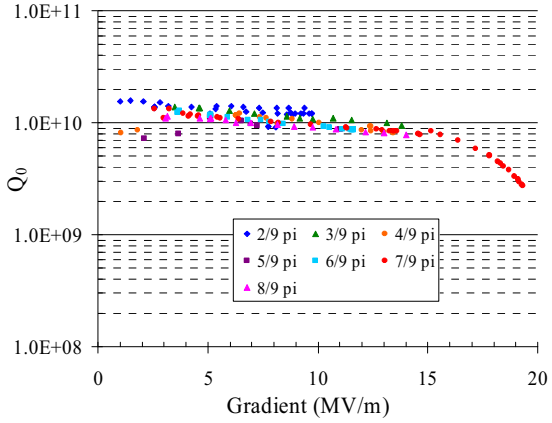

Figure 9: Q_0 vs equivalent gradient measurements for the passband modes of AES01.

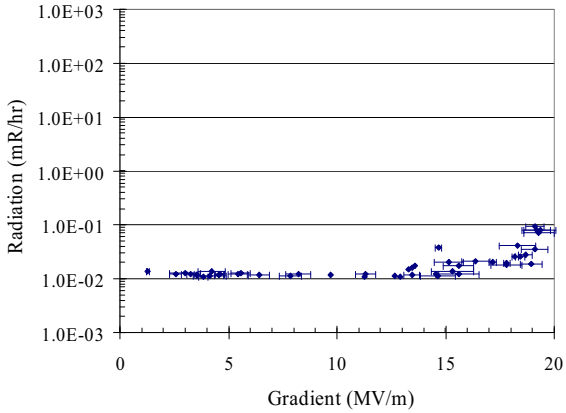

Figure 10: Radiation due to field emission when operating cavity AES01 in the 7π/9 mode

Previous tests at JLab indicated that cells 3/7 were the likely candidates for the source of the cavity's quenches. The field in each cell for the various passband measurements performed in this recent set of tests was determined using calculated field distributions [10] and is shown in Table 2. Inspection of Table 2 confirms that cells 3 & 7 do indeed exhibit the lowest maximum attainable field, which is close to the observed quench field level in the π-mode.

MEASUREMENT ERROR AND ACCURACY

The DAQ and control program used at the Fermilab VCTF, which is essentially identical to that used at JLab [2], calculates measurement errors based on a comprehensive error analysis that takes into account the noise-floor and non-linearity of the power meters, the measured error of the diode detectors, the errors in cable calibrations, the absolute calibration of the reference power meter, and propagation of errors in the performance parameter calculations. Because the decay-based gradient measurement and CW measurement of Q_0 are based on power loss, and the error in power loss

Table 1 : Measurements at maximum limiting field in 2π/9 thru π modes.

Mode	Eacc, max	Freq	Ploss	Q0	U
	(MV/m)	(GHz)	(W)		(J)
2π/9	9.82	1.27790934	8.205	8.42E+09	8.61
3π/9	13.82	1.28125845	20.942	9.49E+09	24.69
4π/9	13.42	1.28542001	23.293	8.04E+09	23.18
5π/9	11.03	1.28996397	14.561	8.70E+09	15.63
6π/9	11.64	1.29412533	16.085	8.60E+09	17.02
7π/9	19.35	1.29763388	142.769	2.73E+09	47.75
8π/9	14.01	1.29996702	26.162	7.80E+09	24.99
π	15.32	1.30081849	26.784	9.12E+09	29.88

Table 2 : Maximum field, in MV/m, in each individual cell for the passband modes.

	Mode							
Cell	π	8π/9	7π/9	6π/9	5π/9	4π/9	3π/9	2π/9
1	16.32	22.61	29.18	16.59	13.40	13.82	10.95	5.62
2	15.14	18.46	14.77	3.16	8.65	17.41	20.20	13.06
3	15.12	13.70	6.43	15.59	15.32	7.59	10.52	14.85
4	15.10	7.35	22.39	15.51	4.25	19.67	10.41	9.80
5	15.09	1.57	28.94	3.16	16.29	3.70	20.20	1.69
6	15.07	7.55	22.22	15.60	4.15	19.64	10.52	9.74
7	15.05	13.87	6.22	15.51	15.38	7.73	10.40	14.83
8	15.03	18.57	14.99	3.12	8.49	17.30	20.18	13.08
9	16.00	22.41	28.98	16.52	13.39	13.87	11.02	5.67

increases dramatically when the reflected power becomes large, it is important to operate the cavity with a near critically-coupled input coupler ($0.5 \leq \beta \geq 2.0$). The error calculations assume that the loop phase is optimized for minimum reflected power, which coincides with maximum transmitted power, otherwise the uncertainty of the calculations increases. Additionally, by reducing the reflected power through phase optimization, errors in the power loss calculation are minimized.

When performing field decay measurements it is important that the crystal detectors not be operated outside of their square-law regime, which must be determined empirically for each specific detector used. Also, it is important that Q_L not vary during the time when the field decay time constant is being determined – this can occur as the result of field emission loading or strong Q-slope. If this were to happen, a systematic error could arise that would lead to calculated values of Q_0 and E that are larger than actual. This can be prevented by using only this first 5-10% of the field decay in order to determine the decay constant τ, and also by only utilizing this technique at lower gradients. Both of these precautions are routinely adopted at the Fermilab VCTF.

CONCLUSIONS

Successful tests of single cell and nine-cell ILC style cavities have been performed at the Fermilab VCTF facility, with results that are in excellent agreement with those obtained at JLab. The RF & DAQ systems performed as designed and required minimal optimization, primarily due to the extensive bench-testing and characterizations performed earlier, the operational tests performed with a Cu cavity at room temperature, and the decision to adopt a well-tested and robust design. Furthermore, the RF & DAQ system of the VCTF had no difficulty in performing mode measurements of the cavity with a fixed input probe which was close to critically coupled ($Q_{ext} = 1.7 \times 10^{10}$) in the π-mode ($\beta \sim 0.8$). The VCTF is prepared to take part in ILC S0 task force infrastructure qualification and cross-calibration activities.

Use of the Fast Thermometry System (FTS) system has allowed the origin of the 15.6MV/m quench in AES01 to be localized to cell 7, and to a specific location just above the weld seam, between the location of sensors #3 & #4, closer to sensor #3. This provides opportunities to pursue additional efficiently targeted investigations.

ACKNOWLEDGMENTS

The authors are grateful to the technical staff of Fermilab's Technical Division Test & Instrumentation department, for their tireless efforts in bringing the VCTF to reality, and for enthusiastically supporting its initial operations, and gratefully acknowledge the efforts of the technical staff of Fermilab's Technical Division SRF Development department for their support. We also would specially like to thank P. Kneisel, R. Geng, C. Reece, and the SRF Department support staff of Jefferson Lab for their assistance in the loan and preparation of the cavities used in these initial tests.

REFERENCES

[1] J. P. Ozelis et al., "Design and Commissioning of Fermilab's Vertical Test Stand for ILC SRF Cavities", PAC'07, Albuquerque, New Mexico, June 2007

[2] C. Grenoble, R. Nehring, J. P. Ozelis, T. J. Powers, "RF and Data Acquisition Systems for Fermilab's ILC SRF Cavity Vertical Test Stand", PAC'07, Albuquerque, New Mexico, June 2007

[3] B. Norris et al., "Cryogenic Infrastructure for Fermilab's ILC Vertical Cavity Test Facility", in Advances in Cryogenic Engineering, vol. 51, Plenum Press, New York, 2007

[4] C. M. Ginsburg et al., "Diagnostic Instrumentation for the Fermilab Vertical Cavity Test Facility", paper TUP47, this conference.

[5] T. J. Powers, "Theory and Practice of Cavity RF Test Systems", Proceedings of the 12th International Workshop on RF Superconductivity", Ithaca NY, July 2005.

[6] P. Kneisel et al., "Development of Large Grain Single Crystal Niobium Cavity Technology at Jefferson Lab", in Proceedings of the Single Crystal Large Grain Niobium Workshop, Araxa, Brazil, 2006, AIP Conference Proceedings 927

[7] Advanced Energy Systems, Medford, NY. www.aesys.net

[8] R. Geng et al., "Latest Results of ILC 9-cell Cavities Electropolished and Vertical Tested at JLab", paper WEP28, this conference

[9] D. Orris et al., "Fast Thermometry for Superconducting Cavity Testing", PAC'07 Albuquerque, New Mexico, June 2007.

[10] P. Kneisel and J. Sekutowicz, private communication